JCTC Journal of Chemical Theory and Computation

Förster Energy Transfer and Davydov Splittings in Time-Dependent Density Functional Theory: Lessons from 2-Pyridone Dimer

Espen Sagvolden,*,[†] Filipp Furche,*,[†] and Andreas Köhn[‡]

University of California, Irvine, Department of Chemistry, 1102 Natural Sciences II, Irvine, California 92697-2025, and University of Mainz, Institute of Physical Chemistry, D-55099 Mainz, Germany

Abstract: The Davydov or exciton splitting of vertical excitation energies is commonly used to estimate the excitation energy transfer rate between chromophores. Here we investigate the S_1-S_2 Davydov splitting in 2-pyridone dimer as a function of the monomer separation, R. We assess the ability of various functionals to reproduce the Davydov splitting at finite R predicted by the approximate coupled cluster singles doubles method CC2. While semilocal functionals fail qualitatively because of spurious charge-transfer intruder states, global hybrids with a large fraction of exact exchange, such as BHandH-LYP, reproduce the CC2 splittings within few wavenumbers. We analyze our results by comparison to lowest-order intermolecular perturbation theory in the spirit of Förster and Dexter. At equilibrium hydrogen bond distance, the Förster−Dexter splittings are too small by up to a factor of 2.

1. Introduction

Excitation energy transfer (EET), the direct migration of energy from a donor to an acceptor chromophore, underlies natural and artificial light harvesting. In photosynthesis[1] and light-driven ion pumps,[2] antenna chromophores transfer solar excitation energy to a reaction center by EET. EET is also essential in excitonic solar cells, allowing the migration of excitons to the interface where charge-separation takes place.[3] Fluorescence resonance energy transfer (FRET) has found widespread use in biology, because the R^{-6} dependence of the EET rate on the chromophore distance R may be used as a spectroscopic ruler.[4]

Quantitative prediction of EET rates from first principles is a challenge for electronic structure methods. According to Förster theory,[5] electronic excitation energy can be transferred from one molecule to a neighboring molecule if their excitation energies are nearly degenerate. It is generally assumed that nuclear relaxation of the donor excited elec-

tronic state takes place on a time scale much faster than energy transfer, so the relevant criterion for transfer is nonzero overlap of the donor emission and the acceptor absorption spectra. In his ground-breaking 1948 paper,[5] Förster used intermolecular perturbation theory to derive his well-known result for the EET rate

$$k_{ET} = K|\langle \Psi_{gs}^A \Psi_{ex}^B | \hat{V} | \Psi_{ex}^A \Psi_{gs}^B \rangle|^2 = K\left| \int dr dr' \frac{\rho^A(\mathbf{r})\rho^B(\mathbf{r}')}{|\mathbf{r} - \mathbf{r}'|} \right|^2 \quad (1)$$

where K accounts for the vibrational density of states and Franck−Condon factors. Here, $\rho^A(\mathbf{r})$ and $\rho^B(\mathbf{r})$ are the transition densities of the unperturbed chromophores. $\hat{V}$ is the sum of electron−electron interactions between electrons on opposite subsystems. Ψ_{gs}^A and Ψ_{gs}^B are the unperturbed chromophore ground states, while Ψ_{ex}^B and Ψ_{ex}^B are the excited states. The second equality is only correct at long-range, where Dexter exchange effects become negligible. In case of dimers, the splitting of the degenerate vertical monomer excitation energies is called Davydov splitting,[6] $\Delta\Omega$. The Davydov splitting may be related to the energy transfer rate by first-order degenerate perturbation theory

---

* To whom correspondence should be addressed. E-mail: esagvold@uci.edu (E.S.); filipp.furche@uci.edu (F.F.).

[†] University of California.

[‡] University of Mainz.

$$k_{\mathrm{ET}} \approx \frac{K}{4}|\Delta\Omega|^2 \tag{2}$$

We will consider the vertical splitting between the electronic energy eigenvalues of the two supersystem states evaluated at a common nuclear geometry. This splitting is also often called exciton splitting.

According to eq 1, k_{ET} is proportional to the square of the classical Coulomb (or Hartree) interaction of the transition densities $\rho^A(\mathbf{r})$ and $\rho^B(\mathbf{r})$. Since the transition densities integrate to zero, eq 1 is dominated by a transition dipole–transition dipole (hereafter called dipole–dipole) interaction at long-range, if the monomer excitations are dipole-allowed

$$k_{\mathrm{ET}} = K\left|\frac{\mathbf{p}_A \cdot \mathbf{p}_B - 3(\mathbf{n}\cdot\mathbf{p}_A)(\mathbf{n}\cdot\mathbf{p}_B)}{R^3}\right|^2 + O\!\left(\frac{1}{R^8}\right) \tag{3}$$

where $\mathbf{R}$ is the vector between the centers of the subsystems, $\mathbf{n} = \mathbf{R}/|\mathbf{R}|$, and $\mathbf{p}_{A/B}$ are the monomer transition dipole moments. At shorter range, the dipole–dipole description is incorrect, because higher-order multipole moments,[7] overlap effects,[8] polarization effects, and the effects of exchange of one or more electrons among the subsystems[9] no longer vanish. In intramolecular EET it may also be difficult to uniquely define two subsystems with separate electronic eigenstates.

An alternative route to EET rates is to extract the exciton splitting $\Delta\Omega$ from a supermolecular calculation, bypassing the limitations of intermolecular perturbation theory. The resulting exciton splittings are directly comparable to spectroscopic results. A detailed comparison of the two approaches to EET was presented by Tretiak et al.[10,11]

Time-dependent density-functional theory (TDDFT)[12] lends itself easily both to the transition density interaction approach and the Davydov splitting approach. It would be beneficial to be able to use TDDFT for EET in biological systems because of the favorable relationship between accuracy and computational cost offered by modern TDDFT methods.[13]

Förster theory has been extensively studied. Several questions have been addressed in articles by other authors. In addition to works mentioned above, the spatial locality of an excitation[10] and the effect of molecular bridges linking two chromophores,[7,14] and of solvents[8,15] have been studied. The Davydov-splitting approach in TDDFT has been studied by Hsu et al.[8] in a basis consisting of the subsystem excitations. In the present paper, we will evaluate the performance of common density functional methods in computing the Davydov splitting using the 2-pyridone dimer as an example. The 2-pyridone dimer is an experimentally well-characterized[16–19] representative of a large family of hydrogen bound dimers and DNA base pairs. In section 2, we will give a short introduction to linear response theory in TDDFT. In section 4, we present benchmark results for various functionals as we vary the length of the hydrogen bond linking the two 2-pyridone monomers.

2. Introduction to Linear Response Theory in TDDFT

From linear response theory in TDDFT within the adiabatic approximation, the excitation energies, Ω, are given by the solutions of the symplectic eigenvalue problem[20–22]

$$(\Lambda - \Omega\Delta)|X, Y\rangle = 0 \tag{4}$$

The excitation vectors

$$|X, Y\rangle = \begin{pmatrix} X \\ Y \end{pmatrix} \tag{5}$$

represent Kohn-Sham (KS) transition density matrices, where $X \in L_{\mathrm{virt}} \times L_{\mathrm{occ}}$ and $Y \in L_{\mathrm{occ}} \times L_{\mathrm{virt}}$. Here, L_{occ} is the Hilbert space of occupied orbitals and L_{virt} the Hilbert space of unoccupied ground-state KS-orbitals. The superoperators Λ and Δ are given by

$$\Lambda = \begin{pmatrix} A & B \\ B & A \end{pmatrix} \qquad \Delta = \begin{pmatrix} 1 & 0 \\ 0 & -1 \end{pmatrix} \tag{6}$$

where 1 is the identity matrix

$$A_{ia\sigma,jb\sigma'} = (\varepsilon_a - \varepsilon_i)\delta_{ij}\delta_{ab}\delta_{\sigma\sigma'} + (ia\sigma|jb\sigma') + f^{\mathrm{xc}}_{ia\sigma,jb\sigma'} - c_x\delta_{\sigma\sigma'}(ab\sigma|ij\sigma) \tag{7}$$

$$B_{ia\sigma,jb\sigma'} = (ia\sigma|jb\sigma') + f^{\mathrm{xc}}_{ia\sigma,jb\sigma'} - c_x\delta_{\sigma\sigma'}(ja\sigma|ib\sigma) \tag{8}$$

The labels i and j denote occupied and a and b unoccupied orbitals and $(ia\sigma|jb\sigma')$ is a two-electron repulsion integral in Mulliken notation. $f^{\mathrm{xc}}_{ia\sigma jb\sigma'}$ is given by

$$f^{\mathrm{xc}}_{ia\sigma,jb\sigma'} = \int d\mathbf{r}d\mathbf{r}'\phi_i(\mathbf{r})\phi_a(\mathbf{r})f^{\mathrm{xc}}_{\sigma\sigma'}(\mathbf{r}, \mathbf{r}')\phi_j(\mathbf{r}')\phi_b(\mathbf{r}') \tag{9}$$

Within the adiabatic approximation, the exchange-correlation (xc) kernel $f^{\mathrm{xc}}_{\sigma\sigma'}$ is the second functional derivative of the semilocal part of the chosen xc-functional

$$f^{\mathrm{xc}}_{\sigma\sigma'}(\mathbf{r}, \mathbf{r}') = \frac{\delta^2 E^{\mathrm{xc,sl}}}{\delta\rho_\sigma(\mathbf{r})\delta\rho'_\sigma(\mathbf{r})} \tag{10}$$

c_x is the Hartree–Fock exchange mixing coefficient. In TDHF, $c_x = 1$ and in semilocal functionals it is 0. In global hybrids, it takes values between 0 and 1. The TDDFT-based approach to Davydov splittings of Hsu et al.[8] uses Förster's intermolecular interaction theory. Hsu et al.[8] explore the problem in a basis formed by the local monomer excitations using the isolated monomer KS-eigenvalues and orbitals. They derive their estimate of the Davydov splitting by calculating the first-order perturbation of the excitation energy from the interaction between the subsystems. Their basis includes only local excitations in the monomers (as opposed to charge-transfer excitations between monomers), which are the relevant excitations in Förster theory. This provides a theory correct to the level where either the KS-eigenvalues deviate from the monomer values, the dimer orbitals deviate from linear combinations of pairwise degenerate monomer orbitals or the charge-transfer excitations mix with the local excitations.
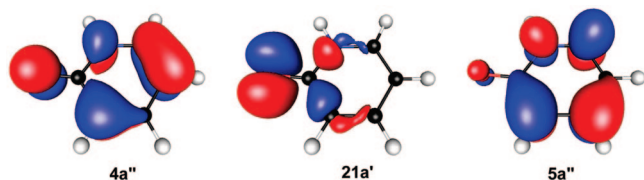
Förster Energy Transfer and Davydov Splittings

J. Chem. Theory Comput., Vol. 5, No. 4, 2009 **875**

Figure 1. Monomer π (4a''), n (21a'), and π^* (5a'')-orbitals. Molecular orbital (MO) plots were generated using a contour value of 0.05 and PBE/aug-def2-TZVP orbitals.

3. Computational Details

Ground-state structures were optimized using second-order Møller−Plesset theory (MP2) within the resolution-of-the-identity (RI) approximation[23−25] and polarized triple-ζ valence (def2-TZVPP)[26] basis sets. The coordinate file is given as Supporting Information. The structure was confirmed to be a minimum by a force constant calculation[27,28] using PBE0[29] and polarized triple-ζ valence (def2-TZVP)[26] basis sets with additional diffuse augmentation from aug-cc-pVTZ.[30] Starting from this geometry, we increased the distance between the monomers by stretching the hydrogen bonds by increments of 1 au and reoptimized the ground-state geometry in C_{2h} keeping the hydrogen bond length fixed. For this set of geometries, vertical singlet excitation energies were computed using the local density approximation (LDA),[31−33] Perdew−Burke−Ernzerhof generalized gradient approximation (PBE),[34] B3LYP global hybrid,[35−38] PBE0 global hybrid,[29] and BHandH-LYP global hybrid[35−37,39] functionals, as well as configuration interaction with single excitations (CIS), time-dependent Hartree−Fock (TDHF) and the approximate coupled cluster singles doubles method CC2.[59,60] The TDHF and CIS calculations were performed using def2-TZVPP[26] basis sets, with diffuse augmentation from aug-cc-pVTZ,[30] CC2 using an aug-cc-pVQZ basis,[30] and the TD-DFT calculations using def2-TZVP[26] basis sets with diffuse augmentation from aug-cc-pVTZ.[30] All calculations were performed using the TURBOMOLE package[40−48] using an m4 grid for DFT calculations. Interaction matrix elements from monomer transition densities were calculated according to eq 1, including exchange and overlap effects where applicable. These calculations were performed using an implementation described in ref 7.

4. Results

4.1. 2-Pyridone Monomer. We found a monomer ground-state structure with C_s symmetry. We computed the monomer vertical excitation energies, transition densities and transition dipole moments at the RI-MP2 ground-state structure. In all computations, the HOMO is the 4a'' orbital (Figure 1). The 5a'' orbital (Figure 1) is the LUMO in all computations with semilocal and hybrid density functionals. In TDHF (and implicitly CC2 and CIS) the 22a' (an oxygen lone pair) orbital is the LUMO. While all hybrid functionals as well as TDHF, CIS and CC2 yield the first A' excitation as the S_1-state, LDA and PBE incorrectly predict the A'' excitation to be S_1. In Table 1 we display the vertical excitation energy and transition dipole moment of the lowest A' excitation of the monomer.

Table 1. Vertical Excitation Energy, ΔE (in eV), and Transition Dipole Moment, μ (in Debye), in the Length Representation and the Assignment of the Lowest A' and A'' Excitations[a,b]

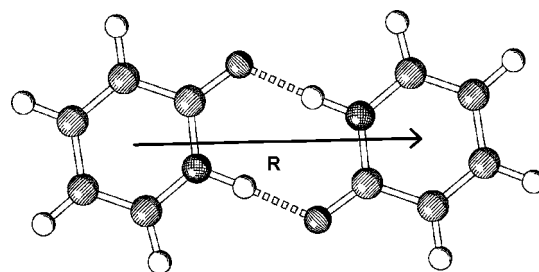|	$2^1A'$			$1^1A''$		
	ΔE	μ	assignment	ΔE	μ	assignment
LDA	3.99	2.00	$\pi \to \pi^*$	3.53	0.09	$n \to \pi^*$
PBE	3.99	2.00	$\pi \to \pi^*$	3.58	0.09	$n \to \pi^*$
B3-LYP	4.26	2.33	$\pi \to \pi^*$	4.44	0.10	$n \to \pi^*$
PBE0	4.35	2.37	$\pi \to \pi^*$	4.60	0.11	$n \to \pi^*$
BHandH-LYP	4.58	2.67	$\pi \to \pi^*$	5.40	0.36	$\pi \to C(3s)$
TDHF	4.89	3.00	$\pi \to \pi^*$	5.73	0.42	$\pi \to C(3s)$
CIS	5.19	3.39	$\pi \to \pi^*$	5.74	0.43	$\pi \to C(3s)$
CC2	4.36	2.50	$\pi \to \pi^*$	4.54	0.04	$n \to \pi^*$
CASPT2[a]	4.37	n/a	$\pi \to \pi^*$	4.99	n/a	$n \to \pi^*$
MRCI-Q[b]	4.70	n/a	$\pi \to \pi^*$	n/a	n/a	n/a

[a] Ref 49. [b] Ref 50.

Figure 2. Structure of the 2-pyridone dimer. We will use two length scales in this article. The distance, R, between the centers of the monomers, as defined above, and the elongation of the hydrogen bond relative to its equilibrium value (in integer steps from 0a.u. to 8a.u.). At the equilibrium structure, $R = 11.15$ au.

The $\pi \to \pi^*$ transition giving rise to the lowest A' excitation is almost a pure 4a''→5a'' transition in TDDFT. In CC2, however, is it dominated by 4$a'' \to$ 6a'' and some weight of 4$a'' \to$ 7a''. This is in keeping with the MRCI-Q results reported by Barbatti et al.[50] With CIS and TDHF, the 4$a'' \to$ 5a'' transition gets approximately the same weight as the 4$a'' \to$ 6a'' transition.

The lowest A'' excitation is dominated by the 4$a'' \to$ 22a' transition in TDHF and CIS. In CC2, it is dominated by 21$a' \to$ 6a'' with some 21$a' \to$ 7a'. In all TDDFT computations, the lowest A'' excitation is almost purely 21 $\to$ 5a'', except BHandH-LYP, where there is also some degree of 21$a' \to$ 6a''.

4.2. 2-Pyridone Dimer Ground-State and Vertical Excitations. The RI-MP2 ground-state structure of the 2-pyridone dimer was found to have C_{2h} symmetry and is displayed in Figure 2. Monomer states of A' symmetry split into dimer eigenstates with A_g and B_u symmetry, while the monomer states of A'' symmetry split into A_u and B_g states. The lowest A_g and B_u excitation energies are given in Table 2. On the basis of the monomer computations, methods predicting the lowest monomer A' transition to be 4$a'' \to$ 5a'', should predict that the lowest A_g and B_u transitions are transitions between the occupied states 4a_u and 4b_g and the virtual states 5a_u and 5b_g. This turns out to be the case. Likewise, the CC2 excitation is dominated by transitions from 4a_u and 4b_g into 6a_u and 6b_g.

Table 2. Vertical Excitation Energy, ΔE (in eV), and Transition Dipole Moment, μ (in Debye) of the 2-Pyridone Dimer[a]

	2^1A_g		1^1B_u	
	ΔE	μ	ΔE	μ
LDA	3.348	0.00	3.382	0.65
PBE	3.371	0.00	3.403	0.62
B3-LYP	4.176	0.00	4.333	0.70
PBE0	4.328	0.00	4.511	3.05
BHandH-LYP	4.616	0.00	4.752	3.47
TDHF	4.936	0.00	5.062	3.89
CIS	5.226	0.00	5.375	4.44
CC2	4.290	0.00	4.426	3.23

[a] All excitations have $\pi \rightarrow \pi^*$ character.

Table 3. Davydov Splitting between the Lowest Singlet A_g Excitation and the Lowest Singlet B_u Excitation at Different Values of the Elongation of the Hydrogen Bonds[a]

method	0 au	1 au	2 au	3 au	4 au	5 au	6 au	7 au	8 au
LDA	278	53	10	2	0	0	0	0	0
PBE	259	50	9	2	0	0	0	0	0
B3-LYP	1266	629	423	291	209	159	125	100	82
PBE0	1480	727	428	292	214	164	130	104	85
BHandH-LYP	1101	716	493	356	267	208	165	134	110
TDHF	1019	745	544	408	314	248	200	163	135
CIS	1205	897	662	500	387	306	247	202	167
CC2	1099	682	456	323	239	183	144	115	93

[a] Distances in a.u. relative to the equilibrium bond length. Note that the lowest singlet excited states for LDA and PBE are charge transfer states, not the localized excitations we are studying. All splittings in cm^{-1}.

For symmetry reasons, the A_g excitations are dipole forbidden and the transition dipole moment of the B_u state should be roughly $\sqrt{2}$ times the transition dipole moment of the monomer A' excitation. As can be seen from comparison of Tables 1 and 2, this is true for PBE0, BHandH-LYP, TDHF, CC2, and CIS, but not for B3-LYP, PBE, and LDA. As will be discussed below, this is due to an admixture of charge-transfer excitations into the local excitations in the case of B3-LYP and the incorrect ordering of local and charge transfer excitations with semilocal functionals.

4.3. Dimer Davydov Splittings. We will now investigate how the design of a density functional affects the splitting at ranges where chromophores (in this case the 2-pyridone monomers) are separated by several au. This is an important regime, both to real cases of energy transfer in nature and to the application of energy transfer as a spectroscopic ruler.

The calculated Davydov splittings of the 2^1A_g and 1^1B_u are displayed in Table 3 and Figure 3. An experimental value for the Davydov splitting is reported for the dimer in the gas phase. Müller et al.[19] found a splitting on the order of 40−50 cm^{-1}. This value, however, refers to a vibronically resolved spectrum and cannot easily be related to the splitting of vertical excitation energies, as considered here. Strong relaxation effects seem to play a role and warrant further investigations which are beyond the scope of the present work. As benchmark, we use results from CC2 calculations, which is the most accurate level of theory that is applicable to a system of the present size. CC2 yields accurate excitation energies for systems with single reference ground states. The
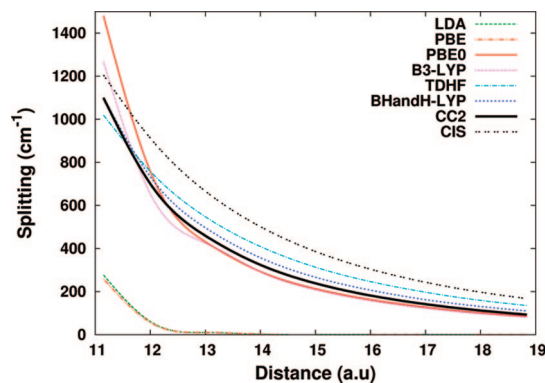
Figure 3. Decay of the Davydov splitting calculated by different methods. Splittings in cm^{-1}. R is the distance between the centers of the two monomers, the equilibrium distance is 11.15 au.
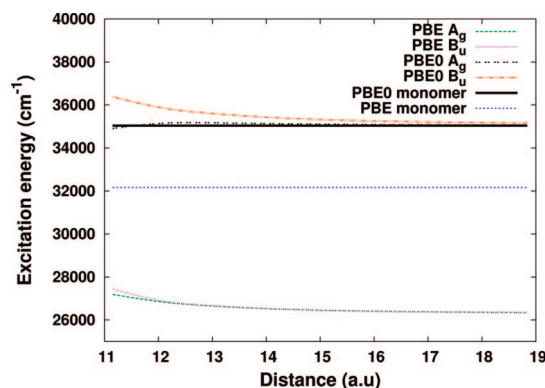
Figure 4. Decay of the first splitting calculated by PBE and PBE0 in cm^{-1}. One sees that while the PBE dimer excitation energies are far away from the PBE monomer first excitation energy, the PBE0 dimer excitation energy tends to its monomer excitation energy as the range increases. This indicates that the lowest PBE0 excitation is local while that of PBE is a charge-transfer excitation. LDA (not displayed) has the same behavior as PBE.

D_1 diagnostic of Janssen and Nielsen[51] is in the range of 0.07−0.08, indicating that CC2 should be reliable here. Furthermore, the T_2 measure for double excitations is in the area of 8−10%. This is also indicative that we should be able to rely on the CC2 calculations.

The global hybrid functional BHandH-LYP($c_x = 0.5$) predicts the Davydov splitting accurately within the entire tested range. TDHF($c_x = 1$) fares well at the equilibrium hydrogen bond length but overestimates the splitting as the hydrogen bonds are stretched. B3-LYP($c_x = 0.20$) and PBE0($c_x = 0.25$) overestimate the splitting at the equilibrium hydrogen bond length but perform better when the hydrogen bond is stretched. One can clearly see the dependence of the splitting on the Hartree−Fock mixing coefficient c_x. As the distance between the monomers increases to 8 au greater than the equilibrium distance, one can observe a clear tendency toward increased splitting with respect to c_x going from B3-LYP to PBE0, BHandH-LYP, and TDHF.

LDA and PBE, however, fail completely to predict the correct splitting. Already at the equilibrium distance the splitting between the lowest A_g and B_u states is significantly

Förster Energy Transfer and Davydov Splittings

J. Chem. Theory Comput., Vol. 5, No. 4, 2009 **877**

Table 4. Oscillator Strength f (Length Representation) and Excitation Energy ΔE (in eV) for the Two Lowest Pairs of Singlet Excited States Evaluated When the Hydrogen Bond Has Been Stretched by 8 au

	f			ΔE		
excitation	LDA	PBE	PBE0	LDA	PBE	PBE0
2^1A_g	0	0	0	3.24	3.27	4.35
3^1A_g	0	0	0	3.99	3.99	4.75
1^1B_u	5×10^{-8}	7×10^{-8}	0.18	3.24	3.27	4.36
2^1B_u	0.12	0.12	4×10^{-7}	4.00	4.00	4.75

Table 5. Energy of 2^1B_u Minus the Energy of the 3^1A_g in cm^{-1}[a]

method	0 au	1 au	2 au	3 au	4 au	5 au	6 au	7 au	8 au
LDA	260	364	286	208	153	116	90	71	58
PBE	291	368	286	207	153	116	91	72	58
PBE0	−678	−155	−28	−5	−1	0	0	0	0

[a] This is the LDA and PBE predictions for the Davydov splitting between the localized excited states. The PBE0 states shown are charge transfer excitations. The splitting for PBE at 4 au failed to converge.

less than for the other functionals, and from there the splitting rapidly falls off to zero as the hydrogen bond length is stretched.

The reason for this discrepancy is that the first excited-state in the LDA and PBE calculations is not the localized excitation, but rather the corresponding charge-transfer (CT) excitation. It is well-known[52,53] that both Hartree−Fock, semilocal density functionals and their hybrids will estimate the energy of CT excitations to be the Kohn−Sham gap $\varepsilon_{LUMO} - \varepsilon_{HOMO}$ at large R, while the correct excitation energy in the large R limit is the monomer excitation energy. For semilocal functionals, the Kohn−Sham gap is generally lower than the actual charge transfer excitation energy.[54] The PBE HOMO−LUMO gap at 8 au is 3.27 eV and the LDA gap is 3.24 eV, which coincides with the excitation energies of the 2^1A_g and 1^1B_u states given in Table 4. Both for LDA and PBE, the excitation energy of the 3^1A_g state is 3.99 eV and that of the 2^1B_u state is 4.00 eV, close or identical to the monomer excitation energies reported in Table 1. Also, the oscillator strength of a long-range charge-transfer excitation is negligible because of the vanishing overlap between eigenstates centered on opposite systems. We observe that for LDA and PBE, the oscillator strength for the transition to 1^1B_u is close to zero, while that of the transition to 2^1B_u is not. In contrast, for PBE0 the excitation energy of the 2^1A_g and 1^1B_u states equal the vertical excitation energy to the $2^1A'$ state of the monomer and the oscillator strength of the 1^1B_u transition is not small. We conclude that in LDA and PBE, the first pair of excitations are spurious charge transfer excitations, while the local excitations relevant to our investigation is the second pair of excitations. Table 5 displays the splitting of the second pair of excited states, showing the relevant Davydov splitting predicted by LDA and PBE.

However, even in the case of B3-LYP and PBE0, there is significant admixture of the CT excitations into the lowest excitations at short-range. At long-range, the dimer molecular
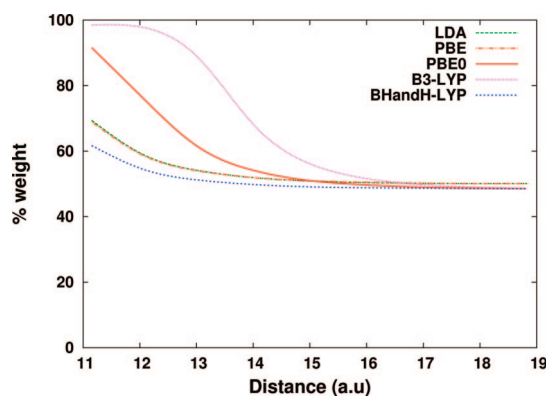
Figure 5. Weight of the dominant configuration in the 2^1A_g excitation as a function of the distance, R, between the centers of the monomers.

orbitals are linear combinations of pairs of degenerate monomer orbitals, and

$$|a''_{A/B}\rangle = \frac{1}{\sqrt{2}}(\langle a_u \rangle \pm \langle b_g \rangle) \qquad (11)$$

Here, $|a''_{A/B}\rangle$ denotes a monomer orbital in the a'' irreducible representation (IRREP) of C_s and $|a_u\rangle$ and $|b_g\rangle$ are the corresponding dimer orbitals in the a_u and b_g IRREPs of C_{2h}. If the monomer $S_0 \rightarrow S_1$ excitation is a pure $4a'' \rightarrow 5a''$ transition, the TDDFT excitation vector for the resulting A_g dimer state has the form

$$
\begin{aligned}
|^1A_g\rangle_{loc} &= \frac{1}{\sqrt{2}}(|4a''_A\rangle\langle 5a''_A| + |4a''_B\rangle\langle 5a''_B|) \\
&= \frac{1}{\sqrt{2}}(|4a_u\rangle\langle 5a_u| + |4b_g\rangle\langle 5b_g|)
\end{aligned} \qquad (12)
$$

for a local excitation and

$$
\begin{aligned}
|^1A_g\rangle_{CT} &= \frac{1}{\sqrt{2}}(|4a''_A\rangle\langle 5a''_B| + |4a''_B\rangle\langle 5a''_A|) \\
&= \frac{1}{\sqrt{2}}(|4a_u\rangle\langle 5a_u| - |4b_g\rangle\langle 5b_g|)
\end{aligned} \qquad (13)
$$

for a CT excitation. This is similar for the B_u states. Thus, the local and CT excitations are plus and minus linear combinations of *two* dimer configurations with 50% weight each. The deviation of the weight of the dimer configurations from 50% thus implies the admixture of CT character into the local excitation and vice versa.

In Figure 5 and Figure 6 we have plotted the weight of the dominant configuration in the excitations into the 2^1A_g and 1^1B_u states, respectively. The graphs for PBE and LDA stay close to 50% at all ranges. This means that the excitations into their 2^1A_g and 1^1B_u states have pure charge transfer character at all ranges. Likewise, the graphs for BHandH-LYP display the same behavior. However, in this case the excitations into the 2^1A_g and 1^1B_u states have purely local character. The behavior of PBE0 and B3-LYP is different. In the case of the excitation into 2^1A_g, a single configuration has a large weight in PBE0 and yet more so in B3-LYP when the monomers are not too far apart, indicating a large admixture of CT character. As the distance
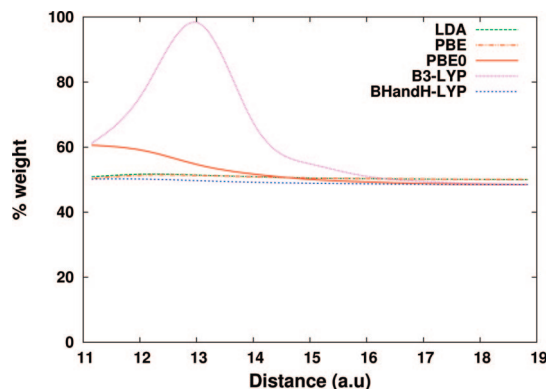
Figure 6. Weight of the dominant configuration in the 1^1B_u excitation as a function of R.

Table 6. Splitting, $\Delta\Omega$ (cm^{-1}), at 8 au from our TDDFT Calculations Compared to Twice the Full Transition Density Interaction (V_{12}^{AB}, Calculated Using Eq 1) and Twice the Dipole-Dipole Interaction (Labeled dip-dip)[a]

method	$\Delta\Omega$	$2 V_{12}^{AB}$ (Coul+exch)	$2 V_{12}^{AB}$ (Coul only)	2 dip-dip	monomer dipole
LDA	58	n/a	n/a	34	0.784
PBE	58	n/a	n/a	35	0.784
B3LYP	82	81	81	51	0.914
PBE0	85	84	84	53	0.931
BHandH-LYP	110	109	109	70	1.049
TDHF	134	135	135	89	1.177

[a] The column labeled (Coul only) contains only the Coulomb interaction between the transition densities. The (Coul+exch) column contains also the exchange part. Also displayed is the size of the monomer transition dipole moment in au.

Table 7. Splitting, $\Delta\Omega$ (cm^{-1}), at 0 au from our TDDFT Calculations Compared to Twice the Full Transition Density Interaction (V_{12}^{AB}, Calculated Using Eq 1) and Twice the Dipole−Dipole Interaction (Labeled dip-dip)[a]

method	$\Delta\Omega$	$2 V_{12}^{AB}$ (Coul+exch)	$2 V_{12}^{AB}$ (Coul only)	2 dip-dip	monomer dipole
LDA	260	n/a	n/a	169	0.734
PBE	291	n/a	n/a	170	0.733
B3LYP	1266	566	636	252	0.877
PBE0	1480	596	668	264	0.897
BHandH-LYP	1101	769	856	348	1.031
TDHF	1019	909	992	451	1.175

[a] The column labeled (Coul only) contains only the Coulomb interaction between the transition densities. The (Coul+exch) column contains also the exchange part. Also displayed is the size of the monomer transition dipole moment in au.

between the monomers increases, they fall off to 50%, meaning that the transition has acquired almost purely local character. For PBE0 the excitation into 1^1B_u appears to be purely local at all ranges based in Figure 6. However, the B3-LYP curve starts at close to 60% at the equilibrium distance, then jumps up to close to 100% when the monomers have been pulled 2a.u. apart and then returns to 50%. This avoided crossing behavior might indicate that the excitation into 1^1B_u at the dimer equilibrium structure is incorrectly predicted to be a charge transfer state by B3-LYP. This is also supported by the low dimer transition dipole moment 1^1B_u reported for B3-LYP in Table 2. As the monomers are pulled apart, it then appears that an even admixture of charge transfer and local excitations arises. At long-range, the local excitation is below the charge transfer excitation. In particular for B3-LYP, the excitations into 2^1A_g and 1^1B_u do not have corresponding weights of local excitations before the hydrogen bond has been stretched approximately 4 au For PBE0, both excitations become purely local at smaller range. The different extent of configuration mixing in PBE0 and B3-LYP rationalizes the bump in the B3-LYP graph in Figure 3 for values of R between 11 au and 13 au.

4.4. Intermolecular Perturbation Theory. Förster's dipole−dipole expression goes as $1/R^6$, with the separation distance R between the chromophores. This is not so at shorter range, however, where higher order transition multipole interactions (which give terms which go as $1/R^8$, $1/R^{10}$, etc.) and Dexter exchange start playing a role. Fückel et al.[7] found for another system that the dipole−dipole approximation was accurate for distances in excess of approximately 50 Å. The Davydov splitting approach also predicts the same $1/R^6$ long-range decay since the splitting goes like $1/R^3$ at long-range. Figure 3 shows the splitting of each method relative to the distance between the centers of the two monomers. Using eq 1, we have calculated the full Coulomb interaction between the monomer transition densities, V_{12}^{AB}, at the equilibrium hydrogen bond length (Table 7) and when it has been stretched 8 au (Table 6). Even when the hydrogen bonds are 8 au longer than their equilibrium length, one observes a significant discrepancy (approximately a factor 2/3) between the splitting calculated from the dipole−dipole interaction and the splitting from the supermolecular calculation. Hence, the dipole−dipole term is insufficient at this range. This is in keeping with the findings of Fückel et al.[7]

However, the splitting appears to be very well described by the full Coulomb interaction of monomer transition densities, while Dexter exchange does not appear to play any significant role at this range. Hence, using the interaction of transition densities appears sufficient at this range. This also implies that, at this range, the ability of a functional to correctly predict the Davydov splitting is determined exclusively by its ability to correctly reproduce the monomer transition density.

As we can see from Table 7, however, at equilibrium distance there is a dramatic discrepancy between the splitting as predicted by the transition densities of the monomers and the splitting from the supermolecular calculations. This is a regime where exact exchange in the functional matters, so it is reasonable that including exchange would improve the splittings from the monomer calculations. However, Dexter exchange makes the already-too-small splitting even smaller. It would seem reasonable to assume that since the monomer geometry does not change much as one stretches the hydrogen bond, this is not due to a qualitative change in the ability of functionals to predict the transition densities. Likely, first-order perturbation theory is insufficient at the dimer equilibrium structure. Higher-order effects, such as induction, begin to play a role, as well as nonvanishing overlap of the monomer wave functions. Accounting for all these effects is cumbersome, and convergence of the perturbation series is not guaranteed. The breakdown of intermolecular perturbation theory calls into question the equivalence between the exciton splitting method and För-

ster's transition density interaction at a more fundamental level than the mere insufficiency of the dipole−dipole interaction or the neglect of exchange. Thus, even in the hydrogen-bonded pyridone dimer, the chromophore interaction is too strong for a perturbative treatment in Förster's spirit.

Fink et al.[55] have studied EET between two benzene molecules. They found that TD-DFT with B3-LYP suffered from the same problem of intruder charge-transfer excitation states as we found in our computations only with LDA and PBE. The conclusion of ref 55 was thus that TDDFT was unreliable for EET calculations and that TDHF was the preferable choice. Our present results suggest that this is an overly pessimistic view: Although B3-LYP fails, global hybrid functionals with a larger fraction of exact exchange perform well, while TDHF overestimates the monomer transition dipole moment leading to spuriously large couplings at long-range.

5. Conclusion

We have tested the ability of various modern functionals to correctly predict the Davydov splitting. Semilocal functionals seem unsuitable for routine treatments of the Davydov splitting at realistic chromophore separations because of charge-transfer intruder states, in line with previous observations.[52,55,56] The global hybrid functional BHandH-LYP is in good agreement with splittings calculated with CC2 over the investigated range. We conclude that the method of choice for larger applications is hybrid TDDFT with a large fraction of exact exchange, calibrated by higher level methods such as CC2. Whether range-separated hybrid functionals[57,58] improve on the BHandH-LYP results further remains to be investigated.

There is an observable breakdown of the equivalence between the exciton splitting method and Förster's perturbative approach at equilibrium distance even for the hydrogen-bonded 2-pyridone dimer. We attribute this to the breakdown of first-order degenerate perturbation theory when the coupling becomes too strong. More effort is necessary to develop methods that accurately predict EET rates over the full range of chromophore separations.

Supporting Information Available: RI-MP2/def2-TZVPP ground-state structures of the 2-pyridone monomer and 2-pyridone dimer. This material is available free of charge via the Internet at http://pubs.acs.org.

References

(1) Engel, G. S.; Calhoun, T. R.; Read, E. L.; Ahn, T.-K.; Mancal, T.; Cheng, Y.-C.; Blankenship, R. E.; Fleming, G. R. *Nature* **2007**, *446*, 782.

(2) Balashov, S. P.; Imasheva, E. S.; Boichenko, V. A.; Anton, J.; Wang, J. M.; Lanyi, J. K. *Science* **2005**, *309*, 2061.

(3) Gregg, B. A. *J. Phys. Chem. B* **2003**, *107*, 4688.

(4) Stryer, L.; Haugland, R. P. *Proc. Nat. Acad. Sci.* **1967**, *58*, 719.

(5) Förster, T. *Ann. Phys.* **1948**, *437*, 55.

(6) Kasha, M.; Rawls, H. R.; Bayoumi, M. A. E. *Pure Appl. Chem.* **1965**, *11*, 371.

(7) Fückel, B.; Köhn, A.; Harding, M. E.; Diezemann, G.; Hinze, G.; Basché, T.; Gauss, J. *J. Chem. Phys.* **2008**, *128*, 074505.

(8) Hsu, C.-P.; Fleming, G. R.; Head-Gordon, M.; Head-Gordon, T. *J. Chem. Phys.* **2001**, *114*, 3065.

(9) Dexter, D. L. *J. Chem. Phys.* **1953**, *21*, 836.

(10) Tretiak, S.; Mukamel, S. *Chem. Rev.* **2002**, *102*, 3171.

(11) Tretiak, S.; Middleton, C.; Chernyak, V.; Mukamel, S. *J. Phys. Chem. B* **2000**, *104*, 4519.

(12) *Time-Dependent Density Functional Theory*; Marques, M., Ullrich, C. A., Nogueira, F., Rubio, A., Burke, K., Gross, E. K. U. , Eds.; Spinger: Berlin, 2006; Vol. 23.

(13) Elliot, P.; Furche, F.; Burke, K. Excited states from time-dependent density functional theory. In *Reviews in Computational Chemistry*; Lipkowitz, K. B., Cundari, T. R. , Eds.; 2009; Vol. 26, p 91.

(14) Russo, V.; Curutchet, C.; Mennucci, B. *J. Phys. Chem. B* **2007**, *111*, 853.

(15) Iozzi, M. F.; Mennucci, B.; Tomasi, J. *J. Chem. Phys.* **2004**, *120*, 7029.

(16) Held, A.; Pratt, D. W. *J. Am. Chem. Soc.* **1990**, *112*, 8629.

(17) Matsuda, Y.; Ebata, T.; Mikami, N. *J. Chem. Phys.* **1999**, *110*, 8397.

(18) Müller, A.; Talbot, F.; Leutwyler, S. *J. Chem. Phys.* **2000**, *112*, 3717.

(19) Müller, A.; Talbot, F.; Leutwyler, S. *J. Chem. Phys.* **2002**, *116*, 2836.

(20) Casida, M. E. In *Recent Advances in Density Functional Methods, Part I*; Chong, D. P. , Ed.; World Scientific: Singapore, 1995; Vol. 1, Chapter 5, pp 155−192.

(21) Furche, F. *J. Chem. Phys.* **2001**, *114*, 5982.

(22) Furche, F.; Ahlrichs, R. *J. Chem. Phys.* **2002**, *117*, 7433.

(23) Ahlrichs, R. *Phys. Chem. Chem. Phys.* **2004**, *6*, 5119.

(24) Weigend, F.; Häser, M. *Theor. Chem. Acc.* **1997**, *97*, 331.

(25) Weigend, F.; Häser, M.; Patzelt, H.; Ahlrichs, R. *Chem. Phys. Lett.* **1998**, *294*, 143.

(26) Schäfer, A.; Huber, C.; Ahlrichs, R. *J. Chem. Phys.* **1994**, *100*, 5829.

(27) Deglmann, P.; Furche, F.; Ahlrichs, R. *Chem. Phys. Lett.* **2002**, *362*, 511.

(28) Deglmann, P.; Furche, F. *J. Chem. Phys.* **2002**, *117*, 9535.

(29) Perdew, J. P.; Ernzerhof, M.; Burke, K. *J. Chem. Phys.* **1996**, *105*, 9982.

(30) Kendall, R. A.; Dunning, T. H.; Harrison, R. J. *J. Chem. Phys.* **1992**, *96*, 6796.

(31) Dirac, P. A. M. *Proc. Royal Soc. (London) A* **1929**, *123*, 714.

(32) Slater, J. C. *Phys. Rev.* **1951**, *81*, 385.

(33) Perdew, J. P.; Wang, Y. *Phys. Rev. B* **1992**, *45*, 13244.

(34) Perdew, J. P.; Burke, K.; Ernzerhof, M. *Phys. Rev. Lett.* **1996**, *77*, 3865.

(35) Vosko, S. H.; Wilk, L.; Nusair, M. *Can. J. Phys* **1980**, *58*, 1200.

(36) Becke, A. D. *Phys. Rev. A* **1988**, *38*, 3098.

(37) Lee, C.; Yang, W.; Parr, R. G. *Phys. Rev. B* **1988**, *37*, 785.

(38) Becke, A. D. *J. Chem. Phys.* **1993**, *98*, 5648.

(39) Becke, A. D. *J. Chem. Phys.* **1993**, *98*, 1372.

(40) *TURBOMOLE*, version V5−10; TURBOMOLE GmbH: Karlsruhe, Germany, 2008. www.turbomole.com.

(41) Ahlrichs, R.; Bär, M.; Häser, M.; Horn, H.; Kölmel, C. *Chem. Phys. Lett.* **1989**, *162*, 165.

(42) Hättig, C.; Weigend, F. *J. Chem. Phys.* **2000**, *113*, 5154.

(43) Hättig, C.; Köhn, A. *J. Chem. Phys.* **2002**, *117*, 6939.

(44) Hättig, C. *J. Chem. Phys.* **2003**, *118*, 7751.

(45) Hättig, C.; Hellweg, A.; Köhn, A. *Phys. Chem. Chem. Phys.* **2006**, *8*, 1159.

(46) Köhn, A.; Hättig, C. *J. Chem. Phys.* **2003**, *119*, 5021.

(47) Eichkorn, K.; Weigend, F.; Treutler, O.; Ahlrichs, R. *Theor. Chem. Acc.* **1997**, *97*, 119.

(48) Weigend, F.; Häser, M. *Theor. Chem. Acc.* **1997**, *97*, 331.

(49) Sobolewski, A. L.; Adamowicz, L. *J. Phys. Chem.* **1996**, *100*, 3933.

(50) Barbatti, M.; Aquino, A. J. A.; Lischka, H. *Chem. Phys.* **2008**, *349*, 278.

(51) Janssen, C. L.; Nielsen, I. M. B. *Chem. Phys. Lett.* **1998**, *290*, 423.

(52) Dreuw, A.; Weisman, J. L.; Head-Gordon, M. *J. Chem. Phys.* **2003**, *119*, 2943.

(53) Hieringer, W.; Görling, A. *Chem. Phys. Lett.* **2006**, *419*, 557.

(54) Tozer, D. J. *J. Chem. Phys.* **2003**, *119*, 12697.

(55) Fink, R. F.; Pfister, J.; Zhao, H. M.; Engels, B. *Chem. Phys.* **2008**, *346*, 275.

(56) Dreuw, A.; Fleming, G. R.; Head-Gordon, M. *Phys. Chem. Chem. Phys.* **2003**, *5*, 3247.

(57) Yanai, T.; Tew, D. P.; Handy, N. C. *Chem. Phys. Lett.* **2004**, *393*, 51.

(58) Vydrov, O. A.; Scuseria, G. E. *J. Chem. Phys.* **2006**, *125*, 234109.

(59) Christiansen, O.; Koch, H.; Jörgensen, P. *Chem. Phys. Lett.* **1995**, *243*, 409.

(60) Hättig, C. *J. Chem. Phys.* **2003**, *118*, 7751.